

Article

A Theoretical Model to Predict the Critical Hydraulic Gradient for Soil Particle Movement under Two-Dimensional Seepage Flow

Zhe Huang ^{1,2}, Yuchuan Bai ^{1,2}, Haijue Xu ^{1,2,*}, Yufen Cao ^{1,3} and Xiao Hu ²

¹ State Key Laboratory of Hydraulic Engineering Simulation and Safety, Tianjin University, 300350 Tianjin, China; Huangzhe1829@163.com (Z.H.); ychbai@tju.edu.cn (Y.B.); coolyufen@163.com (Y.C.)

² Institute for Sedimentation on River and Coastal Engineering, Tianjin University, 300350 Tianjin, China; huxiao_1008@163.com

³ Tianjin Research Institute for Water Transport Engineering, Ministry of Transport, 300456 Tianjin, China

* Correspondence: xiaoxiaoxu_2004@163.com; Tel.: +86-22-2740-1747

Received: 7 October 2017; Accepted: 26 October 2017; Published: 29 October 2017

Abstract: The soil particle movement under seepage flow is one of the predominant mechanisms responsible for incidents and failures of dams and streambanks. However, little attention has been paid to the critical hydraulic gradient under two-dimensional (2-D) seepage flow. In this study, a theoretical model was established under 2-D seepage flow to predict the critical hydraulic gradients for soil particle movement. In this model, the sediment particle rolling theory was used, while taking into account the relative exposure degree of the soil grains and the seepage direction. The model was validated through qualitative analysis and comparison with previous data, and showed considerable superiority over Terzaghi's model. In addition, the effect of the soil internal instability, implying that the critical hydraulic gradient of unstable soil is lower than that of stable soil, was discussed. Various parameters of the model were also analyzed. The results showed that the seepage direction angle was positively related to the critical gradient, whereas the void and the mean diameter of the soil were negatively related to it. Finally, the model proposes a calculation method for the particle movement initiation probability, which is regarded as a key parameter in the sediment transport model.

Keywords: critical hydraulic gradient; 2-D seepage; soil particle movement; relative exposure degree; theoretical model

1. Introduction

Seepage flow could result in erosion and bank instability through several mechanisms. The soil-water pressure, seepage gradient forces, and the soil particle movement in relation to seepage erosion were the focus of previous studies [1,2]. Among these factors, seepage erosion is the predominant failure mechanism causing incidents in dams and streambanks [3,4], being responsible for approximately 50% of the failures [5,6].

The initiation of seepage erosion in soils has been assessed on the basis of hydraulic criteria, particularly in relation to the critical hydraulic gradient i_c . This parameter is usually defined as the critical condition at which the effective stress of the soil becomes negligible [7]. Apparently, a large number of theoretical and experimental approaches have been used to obtain critical hydraulic gradients in water-retaining structures [8–12]. The critical gradient is generally calculated as the ratio of the buoyant unit weight of soil to the unit weight of water, as established by Terzaghi [8] according to the following Equation (1):

$$i_c = \frac{\gamma_s - \gamma_w}{\gamma_w} (1 - n) \quad (1)$$

In this equation, γ_s is the specific weight of soil, γ_w is the specific weight of water, and n is the porosity. Terzaghi suggested that the critical gradient depends only on the void ratio and on the specific gravity of the solids. However, both in the field and in the laboratory, it has been observed that seepage erosion can initiate at gradients much lower than those determined with Terzaghi's classical approach [6,9,10]. For example, Skempton and Brogan [9] carried out tests with upward flow for unstable soils. They found gradient values from one-third to one-fifth smaller than the theoretical values established by Terzaghi. Critical hydraulic gradients lower than 0.1 have also been observed in the field, for example in the failures of the Herbert Hoover Dike and of the A. V. Watkins Dam [10]. Other parameters have been proposed, for instance i_f , defined by Samani [11] as the critical hydraulic gradient of seepage failure. In addition, Wan and Fell [12] introduced i_{start} and i_{boil} to represent the critical hydraulic gradients for the starting of internal erosion and soil boiling, respectively. However, the critical hydraulic gradients described above are generally used for the conventional one-dimensional upward seepage flow; moreover, the resulting estimates are usually not accurate [6,9,10].

The upward seepage parameters described above can only be used to determine the hydraulic criteria in simple cases. In other circumstances, such as the seepage in streambanks and dams, they are invalid, as the seepage includes both a horizontal and a vertical water flow. The criteria for the seepage in both the vertical and the horizontal directions are still not well understood, although several recent studies have quantified soil properties associated with seepage erosion and piping [1,13–15]. There are few equations that accurately estimate the hydraulic criteria. Howard and McLane [16] introduced a critical shear stress equation based on the balance of forces' moments. The forces on the soil grains comprise the tractive force of cumulative surface flow, the seepage force, and gravity. Another theory was developed by Dune [17], whose equation considered the seepage flow direction [2]. Lobkovsky et al. defined a criterion related to the critical slope [18], which was determined by the critical generalized Shields number for overland flow and the density contrast between the granular material and water. Other criteria, such as the initiation i_{ini} and the failure i_f of landslide dams under different geometrical and hydraulic conditions, were determined by Okeke and Wang [7]. The influences of several factors on the gradients were discussed in their research. The critical hydraulic gradients were studied by Adel et al. [19] through tests with stable and unstable soils (based on the Kenney and Lau's criterion [20]). Wan and Fell found that smaller critical hydraulic gradients apply tendentially to soils in a loose state, rather than to soils in a dense state [21]. Similar conclusions were obtained by Ahlinhan et al. in their experimental investigations [22]. Five soil specimens were examined in their experiments to determine the gradient for vertical and horizontal seepages. The internal stability of the soil was proved to be a decisive factor for the critical gradient. However, only few criteria for the soil particle movement in 2-D seepage have been studied so far; in addition, the influence of various parameters on these criteria also requires further study.

According to the previous studies, the hydraulic criteria are influenced by many soil properties. The soil unit weight [8,10], the friction angle [10], the soil particle size [10,23], the soil grain size distribution [7,21], the coefficient of uniformity [10,24], the stress state [25], and the void ratio [21,22,26] were all shown to influence the critical hydraulic conditions. Despite the wealth of research done so far, few studies have thoroughly examined the influence of the relative position of the soil particles and of the seepage direction on the seepage erosion. The locations of soil particles are completely random, which results in different initiation conditions for different particles. As shown in Figure 1, particle C on the far right of the figure is the particle that will be taken away by the flow most easily. On the other hand, the 2-D seepage flow is inhomogeneous in a seepage field with different flow directions. The seepage forces acting on movable particles are different, causing differences in the initiation of soil particles in a 2-D seepage field. Therefore, a deeper understanding of these two aspects of particle movement is absolutely essential.

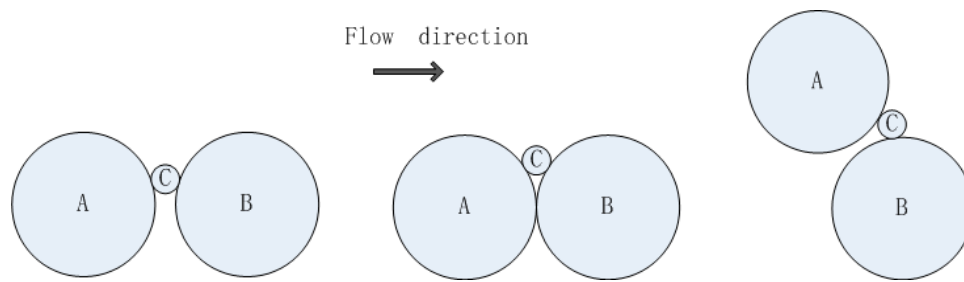


Figure 1. The randomness of particle position.

In this study, a theoretical model was established based on the soil particle rolling theory. In the model, the particles' relative positions and the seepage directions were considered. A calculation formula was derived to predict the hydraulic critical gradients. A qualitative analysis and experimental results demonstrated the formula's validity. The effects of various parameters were discussed, and the particle initiation probability was determined based on the theoretical model.

2. Methods

2.1. Particle Movement Process

The initiation of sediment particles caused by the surface flow can be classified into three different modes: rolling, sliding, and lifting [27]. A previous study showed that the rolling threshold corresponds to the minimum values of the dimensionless critical shear stresses [27]. Particles in the rolling mode present the lowest critical velocity when compared to particles in the other modes. However, in the seepage field, the velocity is generally so small that the rolling condition is relatively easy to achieve. Therefore, in this paper, the rolling mode was assumed to be the initiation process and it was purposely simplified in order to facilitate the ensuing considerations.

2.2. Forces on the Movable Particles

As shown in Figure 2, when the water flows through the soil void, the water force acting on the movable particles (A) is defined as the seepage force (F). The seepage force includes two parts: the drag force and the hydraulic pressure force, resulting from the seepage velocity and the hydraulic gradient, respectively [28]. The seepage force F is determined through the Equation (2) by Wu [29]. The other forces include lift F_L , contact force of motionless particle (B) F_n , friction F_τ , and gravity G . The forces G and F_L are described in Equations (3) and (4).

$$F = \frac{\pi D^2 \rho_W g i (D + e d_{\theta k})}{6} \quad (2)$$

$$G = \frac{\pi D^3 (\rho_S - \rho_W) g}{6} \quad (3)$$

$$F_L = \frac{C_L \rho_W \pi}{2} \frac{\pi}{4} D^2 V_b^2 \quad (4)$$

In the above equations, D is the movable particle diameter, ρ_W and ρ_S are the densities of the water and the soil particles, respectively, g is the gravity acceleration, i is the hydraulic gradient, e is the void ratio of the soil, $d_{\theta k}$ is the equivalent diameter (defined by $1/\Sigma(p_i/d_i)$, where p_i is the percent of grains with the diameter of d_i), C_L is the lift coefficient, and V_b is the seepage velocity in the void. The forces F_n and F_τ have no computational method, and they are obtained from the mechanical equilibrium of a movable particle.

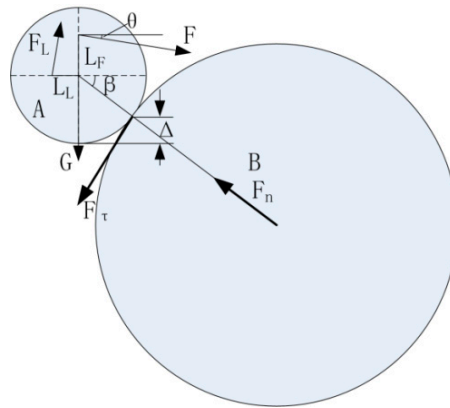


Figure 2. Forces on the movable particles.

2.3. Equilibrium Equations

The critical rolling condition of particle A is a moment equilibrium state. The forces on the movable particles are shown in Figure 2 and represented by Equation (5), in which the moments of F_n and F_τ are equal to zero.

$$G \cdot \cos \beta \cdot R - F \cdot \cos \theta \cdot (L_F + R \cdot \sin \beta) + F \cdot \sin \theta \cdot \cos \beta \cdot R - F_L \cdot \cos \theta \cdot (L_L + R \cdot \cos \beta) - F_L \cdot \sin \theta \cdot \sin \beta \cdot R = 0 \tag{5}$$

In this equation, L_L is the horizontal distance from the center of A to the locus of F_L , L_F is the vertical distance from the center of A to the locus of F ; β is the angle referred to the position of the movable particle, and R is the radius of A. In this study, the forces F_L and F were assumed to be located at the particle center.

2.4. Analysis of the Relative Exposure Degree

The exposure degree Δ , shown in Figure 2, was proposed by Han [30]. It is the vertical distance between the lowest point of the movable particle and the contact point of particle A with the fixed particle B. $\Delta' = \Delta/R$ is the relative exposure degree. In this paper, Δ' was considered to have a uniform distribution from 0 to 1 [31]. The relationships between Δ' and β , shown in Figure 2, are described by the following equations:

$$\sin \beta = \frac{R - \Delta}{R} = 1 - \Delta' \tag{6}$$

$$\cos \beta = \sqrt{1 - (1 - \frac{\Delta}{R})^2} = \sqrt{2\Delta' - \Delta'^2} \tag{7}$$

2.5. Equation for the Critical Hydraulic Gradient

The flow velocity in the seepage field, which is much smaller than in the surface flow, is of the same order of magnitude as the diameters of the sediment particles. Therefore, according to Equations (2)–(4), the magnitude order of the lift force F_L is much lower than that of the seepage force F and of the gravity force G . Thus, the lift force F_L will be ignored in the following sections. The critical hydraulic gradient i_c can be obtained from Equation (5) as follows:

$$i_c = \frac{\rho'}{\rho_w \cos \theta (1 - \Delta') - \sin \theta \sqrt{2\Delta' - \Delta'^2}} \frac{D}{D + ed_{\theta k}} \tag{8}$$

where $\rho' = \rho_s - \rho_w$ is the particle density in water. In Equation (8), the critical hydraulic gradient is influenced by the soil particle density, the movable particle size, the seepage direction, the soil void

ratio, the soil gradation, and the particle relative positions. When the soil parameters are constant, the critical hydraulic gradient varies only with Δ' and θ . Equation (8) can be expressed in a simpler form, as Equation (9)

$$i_c = \Pi \times \Theta \quad (9)$$

where Θ is dependent on the seepage field and the relative exposure degree, as shown in Equation (10), and Π is dependent on the soil parameters, as is shown in Equation (11).

$$\Theta = \frac{\sqrt{2\Delta' - \Delta'^2}}{\cos \theta(1 - \Delta') - \sin \theta \sqrt{2\Delta' - \Delta'^2}} \quad (10)$$

$$\Pi = \frac{\rho'}{\rho_w} \frac{D}{D + ed_{\theta k}} \quad (11)$$

3. Results

3.1. Qualitative Analysis

The seepage inside a slope is not uniform. Generally, the seepage velocity of the slope toe is larger and more prone to seepage erosion. To better characterize it, the critical gradient of the seepage in a slope was analyzed. The distribution of critical hydraulic gradients was calculated through Equation (8). The soil E2 [22] was taken as an example. The specimen in exam can be defined as grit sand, and the hydraulic conductivity can be calculated according to Alyamani and Zekâi [32] as 1.0×10^{-4} m/s, which is consistent with the empirical value in Table 1. The seepage field of a vertical slope model (1 m \times 0.5 m), with water levels of 0.5 m upstream and 0 m downstream, respectively, is shown in Figure 3. The seepage direction θ can be obtained from the seepage field.

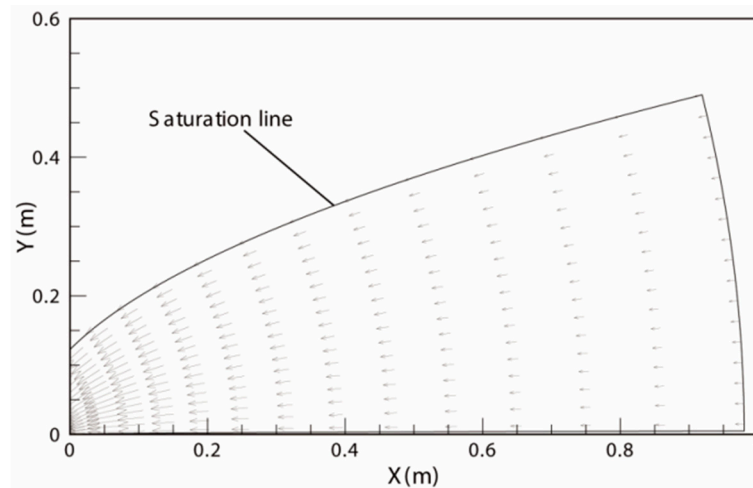


Figure 3. Seepage field of a vertical slope model.

On the basis of previous studies [33], the ratio $d_{c,15}/d_{f,85}$ was used to determine the stability of the soils, with $d_{c,15}$ = grain diameter with 15% w/w of the grains of the coarse soil being finer, and $d_{f,85}$ = grain diameter with 85% w/w of the grains of the fine soil being finer. The finer particles can be removed by the flow easily. As suggested by Kezdi [33], d_{15} is assumed to be the largest movable particle in Equation (8), and, thus, $D = d_{15}$. Figure 4 shows the distribution of the critical hydraulic gradients that were predicted under different relative exposure degrees ($\Delta' = 0.05, 0.1, 0.2$) and different porosities ($e = 0.43, 0.67, 1$).

Table 1. Empirical values of hydraulic conductivity.

Soils	K (m/s)	Soils	K (m/s)
Coarse gravel	$1\sim 2 \times 10^{-3}$	Clay sand	$2 \times 10^{-5}\sim 10^{-6}$
Sandy gravel	$10^{-3}\sim 10^{-4}$	Sandy loess	$10^{-5}\sim 10^{-6}$
Grit sand	$5 \times 10^{-4}\sim 10^{-4}$	Muddy loess	$10^{-7}\sim 10^{-8}$
Silver sand	$5 \times 10^{-5}\sim 10^{-5}$	Clay	$10^{-8}\sim 10^{-10}$

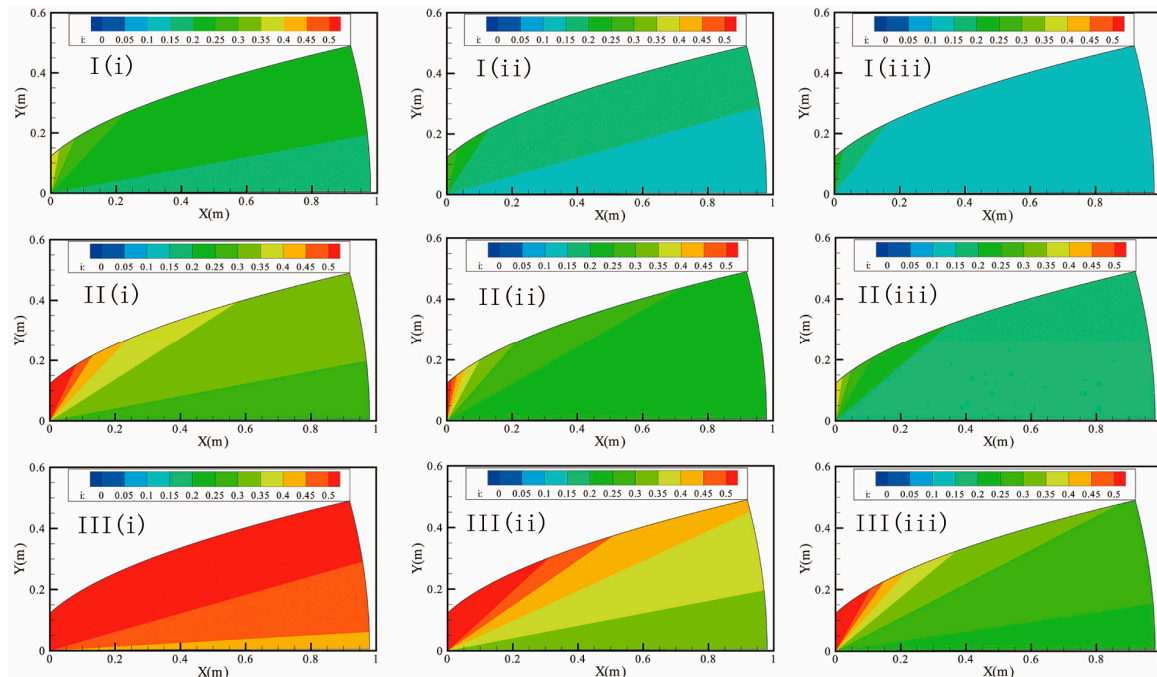


Figure 4. The distribution of the critical hydraulic gradients. In I, II, and III Δ' are 0.05, 0.1, and 0.2, respectively; in (i), (ii), and (iii) e are 0.3, 0.4, and 0.5, respectively.

For the vertical slope shown in Figure 4, the critical hydraulic gradient in the slope toe, where seepage erosion and seepage undercutting in the sand are most likely to happen, as demonstrated by Chu-Agor et al. [1,34], is small. From the toe, up to the top, the critical hydraulic gradient gradually becomes larger. With different Δ' and e , the distributions of the critical hydraulic gradients in the slope are obviously different. More specifically, as Δ' increases, the critical hydraulic gradient will increase and the seepage erosion will occur less likely. On the other hand, as the void ratio increases and the soil becomes less compact, the critical hydraulic gradient will decrease and the seepage erosion will occur more likely.

3.2. Experimental Validation

Experimental data were collected and compared with those predicted by the theoretical model. The predicted i is calculated through Equation (8). In the prediction, the relative exposure degree of d_{15} was set at 0.1 because a few movements of particles can lead to seepage failure. The value of the soil particle density was 2.65 g/cm^3 . According to the analyses above, Equation (8) can be reduced to Equation (12).

$$i_c = \frac{1.65}{2.06 \cos \theta - \sin \theta} \frac{d_{15}}{d_{15} + ed_{\theta k}} \tag{12}$$

The experimental data were obtained from Ahlinhan et al. [22]. In the examined experiment, five different non-cohesive soils were tested in specially developed test devices, under horizontal

seepage flow. The void ratio of the soils varied in the tests. The predicted and experimentally measured data, depicted in Figure 5, matched very well ($R^2 = 0.98$).

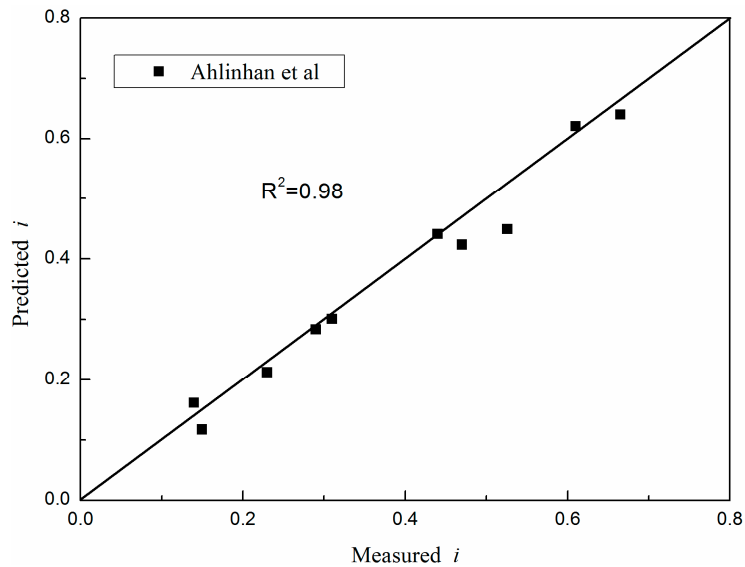


Figure 5. Comparison between predicted and measured data (Ahlinhan’s test).

Another set of experimental data was obtained from Liang et al. [35]. These researchers carried out a series of non-cohesive soil tests, with varying angle model slots. The angles were set as 96° , 100° , 104° , 108° , 112° , and 116° (with the direction of gravity). The critical hydraulic gradients of four groups of particles were measured in the test. The comparison between the predicted data and the measured data is shown in Figure 6.

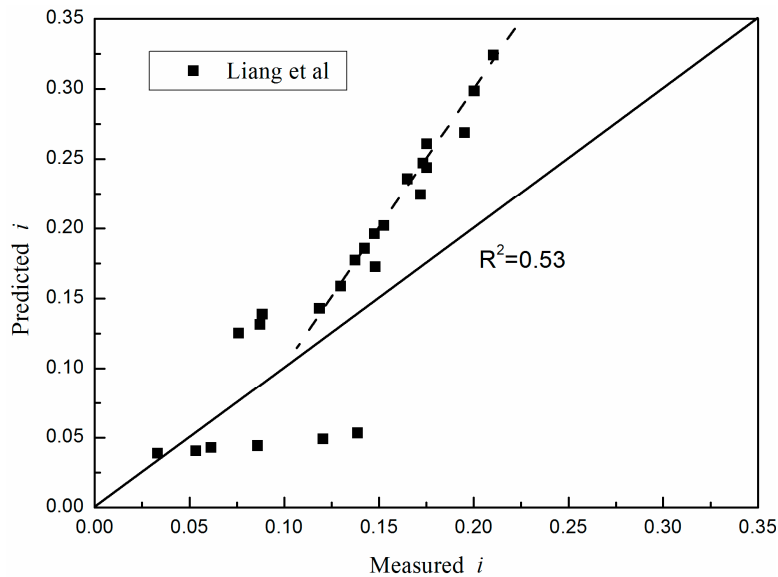


Figure 6. Comparison between predicted and measured data (Liang’s test).

As can be seen from Figure 6, the predicted values did not match with the measured values ($R^2 = 0.53$). The data-points above the solid line indicate that the predicted values were greater than the measured values. This is because the gradients of the soil specimens gradually increased during the test. In smaller gradients, fine particles were removed by the flow, which made the soil much looser.

In a looser soil, the measured gradients are smaller than the real gradients. The points below the line indicate that the predicted i were underestimated. This may result from the obstruction caused by the finer particles, which affects the other particles of the group when the hydraulic gradient is small.

Equation (8) can also be applied to the case of an upward vertical seepage flow. In the vertical seepage flow, the seepage angle θ is equal to -90° , and the parameter Θ is 1. Equation (8) can be simplified to Equation (13).

$$i_c = \frac{\rho'}{\rho_W} \frac{D}{D + ed_{\theta k}} \tag{13}$$

Many studies examined the critical gradient under an upward seepage. The results of three experiments were collected to be compared with the predicted results [9,22,36,37] (Figure 7). Overall, the predicted results and the measured data matched very well ($R^2 = 0.91$), though there was some discrepancies between them. The results from these experiments are presented in Table 2. For the experiment of Ahlinhan et al., the predicted results were more accurate than for the other two experiments. In the Fleshman and Rice’s test, the critical hydraulic gradient was overestimated.

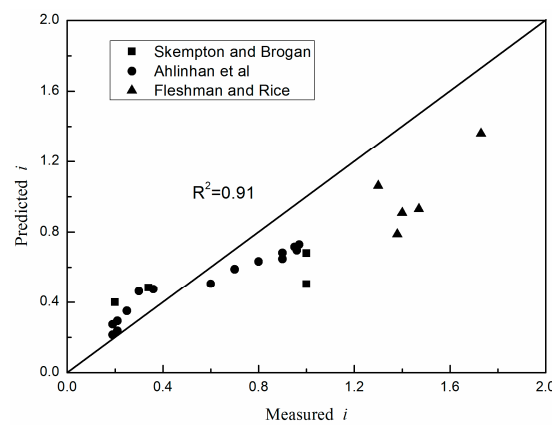


Figure 7. Comparison between predicted and measured data for an upward seepage.

Table 2. Predicted and measured i in the analyzed experiments.

Predicted i	Measured i	Author
0.39	0.20	Skempton and Brogan
0.48	0.34	
0.50	1.00	
0.68	1.00	
0.60	0.70	Ahlinhan et al.
0.63	0.80	
0.71	0.90	
0.73	0.95	
0.70	0.90	
0.72	0.96	
0.75	0.97	
0.42	0.30	
0.43	0.36	
0.52	0.60	
0.25	0.19	
0.24	0.21	
0.31	0.25	
0.21	0.19	
0.23	0.21	
1.10	1.30	Fleshman and Rice
0.93	1.47	
0.91	1.40	
0.81	1.38	
1.36	1.73	

4. Discussion

4.1. Effect of the Soil Internal Instability

The internal instability of the soil is the main factor affecting the critical hydraulic gradient [9]. The theoretical model described in this paper can explain this effect effectively. For the unstable soil, $d_{\theta k}$ is much larger than d_{15} , which leads to a smaller II . Therefore, the calculated critical hydraulic gradient was significantly smaller than that of the stable soil. Our theoretical model also agrees with experimental data found in the literature. In the horizontal seepage, Adel [19] demonstrated that the critical hydraulic gradient for unstable soils should be around 0.2, while in Ahlinhan's test [22], the gradients were between 0.14 and 0.29. In our study, the gradients calculated for unstable soils were between 0.16 and 0.28. For stable soils, Adel [19] showed that the critical hydraulic gradient was about 0.7, while in Ahlinhan's test, it was shown to be between 0.52 and 0.66. Our calculated gradients were between 0.42 and 0.64, and, thus, they were similar to those determined experimentally, with only some deviations. In the vertical seepage, the critical hydraulic gradients were between 0.2 and 0.34 for the unstable soil [9]; in Ahlinhan's test [22], they were between 0.19 and 0.25. According to our calculations, the gradients were between 0.21 and 0.48, and, thus, slightly different from the experimental results, but consistent on the whole. For stable soils, Skempton's [9] experimental critical hydraulic gradient was 1.0, while the values determined by Ahlinhan's [22] were between 0.7 and 0.97, and those found by Fleshman's [36,37] were between 1.3 and 1.73. In our study, the gradients varied from 0.51 to 1.36, thus showing that the range of values for the critical hydraulic gradients is relatively large in this case for different soils. In any case, the gradients' values determined in our study were more accurate than Terzaghi's, which were reported to be higher than the real ones [6]. In our analysis, we could also determine the influence of soil instability on the critical hydraulic gradients. We concluded that the critical hydraulic gradients of unstable soil were lower than those of stable soil.

4.2. Effects of Other Parameters

Other parameters including both hydraulic parameters (seepage angle) and soil parameters (void ratio, gradation) affect the critical hydraulic gradient to different extents. In Liang's test [35], the effect of seepage angle on critical hydraulic gradients has been demonstrated. In our study, the relationship between the seepage angle and the predicted i is shown in Figure 8.

It can be seen that at the same seepage direction angle, the hydraulic gradient at the initiation of the particle increased as the particle size increased. For particles in the same size range, the critical hydraulic gradient was positively correlated with the seepage direction angle, as observed for the experimental results reported in the test. Thus, the critical gradient of the vertical seepage is greater than that of the horizontal flow, as observed by Ahlinhan [22]. The vertical and the horizontal seepages were also studied by Skempton and Adel [9,19], respectively, and similar results were reported. The force analysis of soil particles described above can explain this phenomenon. In the vertical seepage flow, the particles' movements need to overcome the gravity, while, in the horizontal flow, the particles can roll around large particles, moving downstream. In this situation the seepage force does not need to be greater than the gravity, but it has to overcome the gravity's moment. In the case of a small seepage force, the seepage force's moment may be greater than the gravity's moment, as shown by the analysis of the particles' exposure degree. Therefore, soil particles are very easily taken away by the horizontal seepage flow.

The soil parameters are also important for the critical gradients [7,21,22]. The effects of the void ratio e and the mean grain diameter $d_{\theta k}$ on the critical gradients are shown in Figure 9. In this figure, the experimental data were obtained from Ahlinhan's vertical seepage test [22].

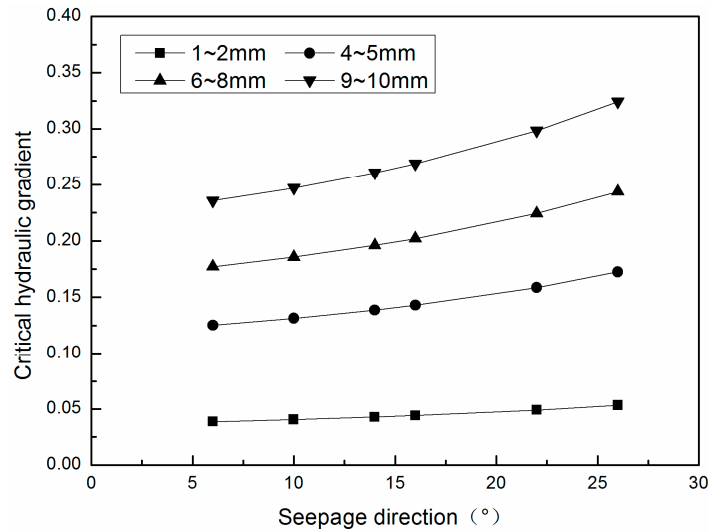


Figure 8. Effects of seepage direction on the critical gradients.

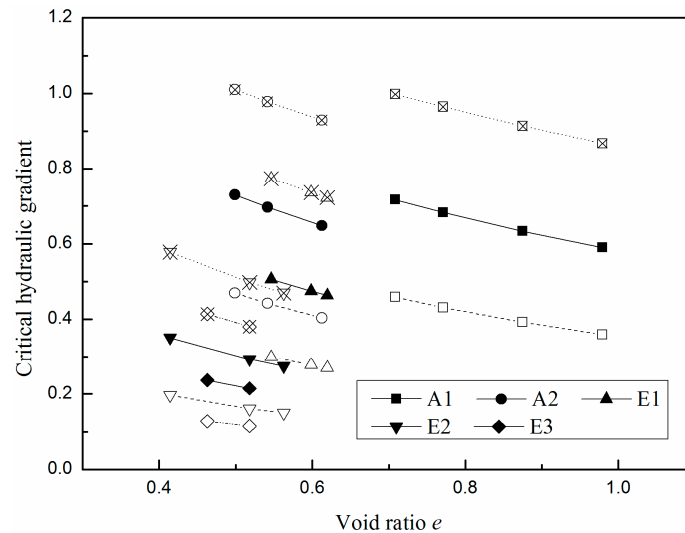


Figure 9. Effects of the soil parameters on the critical gradients.

The dashed lines in Figure 9 denote the relationship between the critical hydraulic gradients and the void ratio after doubling or halving the mean grain diameter of the soil particles. The negative effects of the void ratio on the critical hydraulic gradient are evident, in agreement with Wan and Zhou results [20,38]. Small voids lead to poor mobility of the water flow, which will reduce the removal of soil particles by the water. The values of $d_{\theta k}$ are inversely correlated to those of the critical gradients. Larger $d_{\theta k}$ values indicate that the soil particles are relatively coarse, and the soil is more inhomogeneous and more unstable. This effect is consistent with Skempton and Ahlinhan’s results [9,22].

4.3. Exposure Degree and Particle Initiation Probability

Equation (8) also contains the parameter Δ' . This parameter is a random variable, considered to obey a random distribution, such as a uniform distribution, a normal distribution, a partial normal distribution, etc. [39]. Regardless of the distribution type, the exposure can be obtained through Equation (9), when the particles D can move away in certain hydraulic conditions:

$$\Delta'_0 = F(i, \rho_s, \rho_w, \theta, D, e, d_{\theta k}) \tag{14}$$

The initiation probability of particles D is:

$$p = p(\Delta' \leq \Delta'_0) = \int_0^{\Delta'_0} f(\Delta') d\Delta' \quad (15)$$

where $f(\Delta')$ is the probability density function of Δ' . In Ahlinhan's test [22], for hydraulic gradients of 0.2, 0.4 and 0.6 in a horizontal seepage, the initiation probabilities of soil samples A1 and E1 are shown in Figure 10, assuming that Δ' is uniformly distributed between 0 and 1.

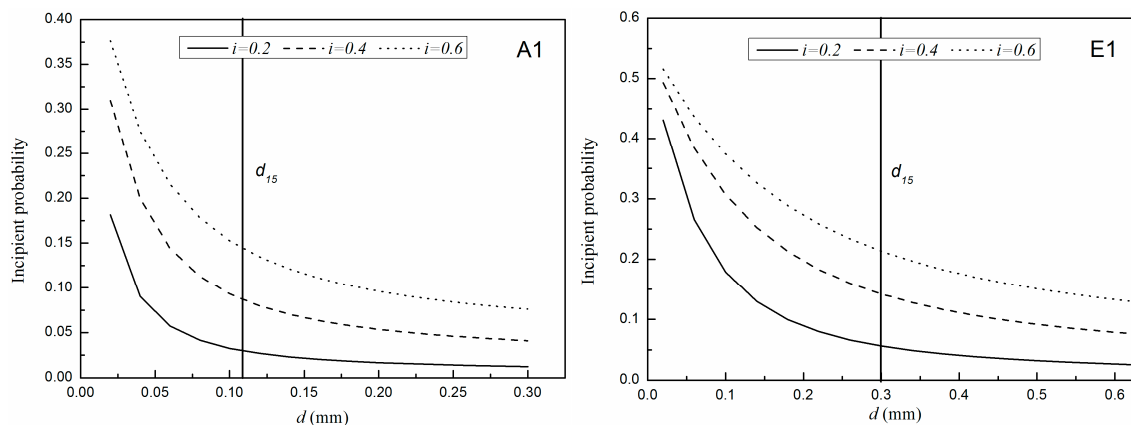


Figure 10. Initiation probability of different particles.

As shown in Figure 10, with the increase of particle size, the initiation probability is gradually reduced, and the decreasing trend gradually becomes smaller. In addition, when the particle size is less than d_{15} , the initiation probability of the particles is large, and the variation is drastic. This suggests that the movable particles are mostly smaller than d_{15} , which, reasonably, represents the largest possible diameter for movable particles. In addition, the initiation probability of the particles is an important factor in the sediment transport studies regarding river dynamics. In the seepage erosion, also the effects of sediment transport need to be determined. Hence, the theoretical model needs to be further developed. The initiation probability determined in this study will allow to develop the theoretical model.

5. Conclusions

The initiation of soil particles is a complex dynamic process influenced by the seepage flow, especially the 2-D seepage flow. Among the multiple factors influencing it, the randomness of sediment particle position and the seepage direction were examined in this study. An equation was established to appraise the critical hydraulic gradient under 2-D seepage flow, based on the basic theory of single-grain rolling movement. By qualitative analysis and comparison with experimental data, our method was demonstrated to be highly accurate in predicting the critical gradient of the 2-D seepage flow.

The results we obtained are considerably more reliable than Terzaghi's. The effects of various parameters on the critical gradients were also discussed. Our results showed that the critical hydraulic gradients of unstable soil were lower than those of stable soil, and that the seepage direction angle was positively related to the critical gradient, whereas the void and the mean diameter of soil were negatively related to it.

This theoretical model was used to determine the initiation probability of particles with an assumed exposure degree distribution. Through the analysis of the initiation probability, the diameter of the movable particles appeared to be, in general, smaller than d_{15} . The initiation probability is a factor contributing to the development of sediment transport under seepage flow.

Acknowledgments: This work was supported by the National Natural Science Foundation of China (No. 41576093, No.51279124, No. 51621092), the Natural Science Foundation of Tianjin (No. 14JZDJC39800) and State Key Laboratory of Hydraulic Engineering Simulation and Safety Foundation (No. HESS-1513).

Author Contributions: Zhe Huang and Haijue Xu conceived the idea and approach for the study. Zhe Huang and Yuchuan Bai analyzed the data. Yufen Cao and Xiao Hu contributed to the language translation. Zhe Huang wrote the paper. All the authors were involved in the preparation of the manuscript.

Conflicts of Interest: The authors declare no conflict of interest.

Notations

β	Angle referred to the position of the movable particle
L_L	Arm of lift force
L_F	Arm of seepage force
F_n	Contact force
i_c	Critical hydraulic gradient
ρ_s	Densities of the soil particles
ρ_w	Densities of the water
$d_{\theta k}$	Equivalent diameter
Δ	Exposure degree
F_τ	Friction force
d_{15}	Grain diameter for which 15% of the grains by weight are finer
$d_{c,15}$	Grain diameter for which 15% of the grains by weight of the coarse soil are finer
$d_{f,85}$	Grain diameter for which 85% of the grains by weight of the fine soil are finer
G	Gravity
g	Gravity acceleration
K	Hydraulic conductivity
i	Hydraulic gradient
i_f	Hydraulic gradient at slopes or dams failure
i_{boil}	Hydraulic gradient at soil boil
i_{start}	Hydraulic gradient at soil starting movement
i_{ini}	Hydraulic gradient at initiation of landslide dams
P	Initiation probability of particles
C_L	Lift coefficient
F_L	Lift force
D	Movable particle diameter
Θ	Parameter referred to the seepage field and the relative exposure degree
Π	Parameter referred to the soil parameters
ρ'	Particle density in water
n	Porosity of the soil
$f(\Delta')$	Probability density function of Δ'
R	Radius of the movable particle
Δ'	Relative exposure degree
θ	Seepage direction
F	Seepage force
V_b	Seepage velocity
γ_s	Specific weight of soil
γ_w	Specific weight of the water
e	Void ratio of the soil

References

1. Chu-Agor, M.L.; Fox, G.A.; Cancienne, R.M.; Wilson, G.V. Seepage caused tension failures and erosion undercutting of hillslopes. *J. Hydrol.* **2008**, *359*, 247–259. [[CrossRef](#)]
2. Fox, G.A.; Wilson, G.V. The role of subsurface flow in hillslope and stream bank erosion: A review. *Soil Sci. Soc. Am. J.* **2010**, *74*, 717–733. [[CrossRef](#)]

3. Hagerly, D.J. Piping/sapping erosion I: Basic considerations. *J. Hydraul. Eng.* **1991**, *117*, 991–1008. [[CrossRef](#)]
4. Wörman, A. Seepage-induced mass wasting in coarse soil slopes. *J. Hydraul. Eng.* **1993**, *119*, 1155–1168. [[CrossRef](#)]
5. Foster, M.; Fell, R.; Spannagle, M. The statistics of embankment dam failures and accidents. *Can. Geotech. J.* **2011**, *37*, 1000–1024. [[CrossRef](#)]
6. Richards, K.S.; Reddy, K.R. Critical appraisal of piping phenomena in earth dams. *Bull. Eng. Geol. Environ.* **2007**, *66*, 381–402. [[CrossRef](#)]
7. Okeke, C.U.; Wang, F. Critical hydraulic gradients for seepage-induced failure of landslide dams. *Geoenviron. Disasters* **2016**, *3*, 1–22. [[CrossRef](#)]
8. Terzaghi, K. Der Grundbruch an Stauwerken und Seine Verhütung. *Wasserkraft* **1922**, *17*, 445–449.
9. Skempton, A.W.; Brogan, J.M. Experiments on piping in sandy gravels. *Géotechnique* **1994**, *44*, 449–460. [[CrossRef](#)]
10. Fleshman, M.S.; Rice, J.D. Constant gradient piping test apparatus for evaluation of critical hydraulic conditions for the initiation of piping. *Geotech. Test. J.* **2013**, *36*, 834–846. [[CrossRef](#)]
11. Samani, Z.A. Soil hydraulic stability in a subsurface drainage system. *Trans. ASAE* **1981**, *24*, 666–669. [[CrossRef](#)]
12. Wan, C.F. *Experimental Investigations of Piping Erosion and Suffusion of Soils in Embankment Dams and Their Foundations*; The University of New South Wales: Sydney, Australia, 2006.
13. Wilson, G.V.; Periket, R.K.; Fox, G.A.; Cullum, R.F. Seepage erosion properties contributing to streambank failure. *Earth Surf. Process. Landf.* **2007**, *32*, 447–459. [[CrossRef](#)]
14. Fox, G.A.; Wilson, G.V.; Simon, A.; Langendoen, E.J.; Akay, O.; Fuchs, J.W. Measuring streambank erosion due to ground water seepage: Correlation to bank pore water pressure, precipitation and stream stage. *Earth Surf. Process. Landf.* **2007**, *32*, 1558–1573. [[CrossRef](#)]
15. Chu-Agor, M.L.; Wilson, G.V.; Fox, G.A. Numerical modeling of bank instability by seepage erosion undercutting of layered streambanks. *J. Hydrol. Eng.* **2008**, *13*, 1133–1145. [[CrossRef](#)]
16. Howard, A.D.; McLane, C.F. Erosion of cohesionless sediment by groundwater seepage. *Water Resources Res.* **1988**, *24*, 1659–1674. [[CrossRef](#)]
17. Dunne, T. Hydrology, mechanics, and geomorphic implications of erosion by subsurface flow. *Spec. Pap. Geol. Soc. Am.* **1990**, *252*, 1–28. [[CrossRef](#)]
18. Lobkovsky, A.E.; Jensen, B.; Kudrolli, A.; Rothman, D.H. Threshold phenomena in erosion driven by subsurface flow. *J. Geophys. Res. Earth Surf.* **2005**, *109*, 357–370. [[CrossRef](#)]
19. Adel, H.D.; Bakker, K.J.; Breteler, M.K. Internal stability of minestone. In *Proceedings of International Symposium of Modelling Soil–Water–Structure Interaction*; Balkema: Rotterdam, The Netherlands, 1988; pp. 225–231.
20. Kenney, T.C.; Lau, D. Internal stability of granular filters. *Can. Geotech. J.* **1985**, *23*, 420–423. [[CrossRef](#)]
21. Wan, C.F.; Fell, R. Assessing the potential of internal instability and suffusion in embankment dams and their foundations. *J. Geotech. Geoenviron. Eng.* **2008**, *134*, 401–407. [[CrossRef](#)]
22. Ahlinhan, M.F.; Achmus, M.; Burns, S.E.; Bhatia, S.K.; Avila, C.M.C. Experimental investigation of critical hydraulic gradients for unstable soils. *Geotech. Spec. Publ.* **2010**, 599–608. [[CrossRef](#)]
23. Ojha, C.S.P.; Singh, V.P.; Adrian, D.D. Determination of critical head in piping. *J. Hydraul. Eng.* **2003**, *129*, 511–518. [[CrossRef](#)]
24. Schmertmann, J.H. The no-filter factor of safety against piping through sands. *Geotech. Spec. Publ.* **2000**, 65–105. [[CrossRef](#)]
25. Chang, D.S.; Zhang, L.M. Critical hydraulic gradients of internal erosion under complex stress states. *J. Geotech. Geoenviron. Eng.* **2013**, *139*, 1454–1467. [[CrossRef](#)]
26. Ojha, C.S.P.; Singh, V.P.; Adrian, D.D. Influence of porosity on piping models of levee failure. *J. Geotech. Geoenviron. Eng.* **2001**, *127*, 1071–1074. [[CrossRef](#)]
27. Choi, S.U.; Kwak, S. Theoretical and probabilistic analyses of incipient motion of sediment particles. *KSCE J. Civ. Eng.* **2001**, *5*, 59–65. [[CrossRef](#)]
28. Marot, D.; Rochim, A.; Nguyen, H.H.; Bendahmane, F.; Sibille, L. Assessing the susceptibility of gap-graded soils to internal erosion: Proposition of a new experimental methodology. *Nat. Hazards* **2016**, *29*, 1–24. [[CrossRef](#)]
29. Wu, L. Computation of the critical hydraulic gradient for piping of non-cohesive soil. *Hydro-Sci. Eng.* **1980**, *4*, 90–95. (In Chinese) [[CrossRef](#)]

30. Han, Q.W.; He, M.M. *Statistical Theory of Sediment Movement*; Science Press: Beijing, China, 1984. (In Chinese)
31. Xu, H.; Shen, Y.; Bai, Y. Statistical analysis on motion characteristics of bedload rolling. *J. Hydraul. Eng.* **2014**, *110*, 1184–1192. (In Chinese) [[CrossRef](#)]
32. Alyamani, M.S.; Zekâi, S. Determination of hydraulic conductivity from complete grain-size distribution curves. *Ground Water* **1993**, *31*, 551–555. [[CrossRef](#)]
33. Kezdi, A. *Soil Physics*; Elsevier Scientific Publishing Company: Amsterdam, The Netherlands, 1979.
34. Chu-Agor, M.L.; Fox, G.A.; Wilson, G.V. Empirical sediment transport function predicting seepage erosion undercutting for cohesive bank failure prediction. *J. Hydrol.* **2009**, *377*, 155–164. [[CrossRef](#)]
35. Liang, Y.; Zhang, Q.; Zeng, C.; Liu, Z. Non-Cohesive Particles Starting Mechanism under the Changing Seepage Direction. *J. Chongqing Jiaotong Univ. (Nat. Sci.)* **2016**, *35*, 89–93. (In Chinese)
36. Rice, J.D.; Fleshman, M.S. Laboratory Modeling of Critical Hydraulic Conditions for the Initiation of Piping. In Proceedings of the Geo-Congress 2013, San Diego, CA, USA, 3–7 March 2013; American Society of Civil Engineers (ASCE): Reston, VA, USA, 2013; pp. 1044–1055.
37. Fleshman, M.S.; Rice, J.D. Laboratory Modeling of the Mechanisms of Piping Erosion Initiation. *J. Geotech. Geoenviron. Eng.* **2014**, *140*, 04014017. [[CrossRef](#)]
38. Zhou, J.; Bai, Y.F.; Yao, Z.X. A mathematical model for determination of the critical hydraulic gradient in soil piping. In Proceedings of the GeoShanghai International Conference 2010, Shanghai, China, 3–5 June 2010; American Society of Civil Engineers (ASCE): Reston, VA, USA; pp. 239–244. [[CrossRef](#)]
39. Xing, R.; Zhang, G.; Liang, Z.; Wu, Z. Study on the location characteristics of bed surface particle. *J. Sediment. Res.* **2016**, *4*, 28–33. (In Chinese) [[CrossRef](#)]



© 2017 by the authors. Licensee MDPI, Basel, Switzerland. This article is an open access article distributed under the terms and conditions of the Creative Commons Attribution (CC BY) license (<http://creativecommons.org/licenses/by/4.0/>).